



Full length article

Transcriptome-wide identification of differentially expressed genes in *Procambarus clarkii* in response to chromium challenge

Xun Meng^{a,b,1}, Liang Hong^{d,1}, Ting-Ting Yang^{a,c,1}, Yu Liu^{a,c,1}, Ting Jiao^a, Xiao-Hua Chu^a, Dai-Zhen Zhang^a, Jia-Lian Wang^a, Bo-Ping Tang^a, Qiu-Ning Liu^{a,***}, Wei-Wei Zhang^{d,*}, Wen-Fei He^{b,**}

^a Jiangsu Key Laboratory for Bioresources of Saline Soils, Jiangsu Synthetic Innovation Center for Coastal Bio-agriculture, Jiangsu Provincial Key Laboratory of Coastal Wetland Bioresources and Environmental Protection, School of Ocean and Biological Engineering, Yancheng Teachers University, Yancheng, 224007, PR China

^b School of Pharmaceutical Sciences, Wenzhou Medical University, Wenzhou, 325035, PR China

^c College of Biotechnology and Pharmaceutical Engineering, Nanjing University of Technology, Nanjing, 210009, PR China

^d Department of Infectious Disease, Ruian People's Hospital, Wenzhou, Zhejiang, 325200, PR China



ARTICLE INFO

Keywords:

Procambarus clarkii
Heavy metal stress
Chromium
Differentially expressed genes
Antioxidant defense system
Transcriptome analysis

ABSTRACT

Because of the high protein content and rich meat quality of crayfish *Procambarus clarkii*, it has become widely popular in China in recent years and has a high economic value. When *P. clarkii* is stimulated by heavy metals, it reacts to oxidation. *P. clarkii* has evolved antioxidant defense systems, including antioxidant enzymes such as catalase (CAT). The hexavalent form of Cr (VI) is a pathogenic factor that is of particular concern in aqueous systems because of its great toxicity to living organisms. In this study, we characterized the transcriptome of *P. clarkii* using a RNA sequencing method and performed a comparison between $K_2Cr_2O_7$ -treated samples and controls. In total, 34,237 unigenes were annotated. We identified 5098 significantly differentially expressed genes (DEGs), including 2536 and 2562 were significantly up-regulated and down-regulated, respectively. In addition, quantitative real time-PCR (qRT-PCR) confirmed the up-regulation of a random selection of DEGs. Our results contribute to a more comprehensive understanding of the antioxidant defense system used by *P. clarkii* in response to heavy metal stress.

1. Introduction

The red swamp crayfish, *Procambarus clarkii*, is native to north-eastern Mexico, North American and South America. It was introduced to China from Japan during the 1930s. The *P. clarkii* is hardy and lives in hostile water environments, including ditches and ponds. Its meat is delicious and has a high protein content. Therefore, the economic value of *P. clarkii* is increasing in China. However, in recent years, an increasing number of factories have been discharging waste water into rivers without any proper treatment; moreover, farmers have been overfertilizing, collectively resulting in serious pollution of the living environment of *P. clarkii*. Heavy metal pollution is the most serious. Cr (VI) is ubiquitous in polluted rivers and can lead to toxicity in *P. clarkii*

[1].

Cr is a toxic metal, and its different forms of oxidation states have been increasingly attracting attention [2]. Its hexavalent form Cr (VI) is an artificial pollutant [3]. Cr (VI) can induce biological acute and chronic toxicity, neurotoxicity, reproductive toxicity, genotoxicity, carcinogenicity, and environmental toxicity [4,5]. Similar to other invertebrates, the crayfish lack an adaptive immune system, being totally dependent on the innate immune system [6]. The innate immune system is the first line of defense against foreign pathogens. The hepatopancreas is an important immune organ and the main synthesis sites of immune-responsive molecules [7]. On exposure to oxidative stress, it secretes antioxidant enzymes, including catalase (CAT), superoxide dismutase (SOD) and glutathione S-transferase (GST) [8].

* Corresponding author. Department of Infectious Disease, Ruian People's Hospital, Wenzhou, Zhejiang, 325200, PR China.

** Corresponding author. School of Pharmaceutical Sciences, Wenzhou Medical University, Wenzhou, 325035, PR China.

*** Corresponding author. Jiangsu Key Laboratory for Bioresources of Saline Soils, Jiangsu Synthetic Innovation Center for Coastal Bio-agriculture, Jiangsu Provincial Key Laboratory of Coastal Wetland Bioresources and Environmental Protection, School of Ocean and Biological Engineering, Yancheng Teachers University, Yancheng, 224007, PR China.

E-mail addresses: liuqn@yctu.edu.cn (Q.-N. Liu), 461357478@qq.com (W.-W. Zhang), wenfei509@163.com (W.-F. He).

¹ These authors contributed equally to this work.

They can remove reactive oxygen species and prevent oxidative damage.

The molecular mechanism underlying the reaction of invertebrates to heavy metals has been a focus of researchers [9,10]. Transcriptome sequencing is widely used in genome analysis and functional gene identification, helping us to understand the genetic response of a host to heavy metal stress and the molecular mechanism underlying antioxidant defense systems [11,12]. Transcriptome studies on a wide variety of invertebrate taxa may provide insights into their innate immune system. The main advantages of RNA sequencing (RNA-seq) technology include good repeatability, wide detection range, high cost-effectiveness, and the ability to provide quantitative expression and activity data [13]. In this study, we used an experimental group treated with $K_2Cr_2O_7$ and a control group treated with phosphate-buffered saline (PBS) to create a transcriptome sequencing library. Differentially expressed genes (DEGs) in different functional databases were analyzed and identified. The transcriptome analysis helped us to reveal the mechanism used by *P. clarkii* to deal with heavy metal stress; our results should be useful for studying genes or pathways related to the metabolism of certain metals by *P. clarkii* [14,15].

2. Materials and methods

2.1. Animal collection and treatment

P. clarkii was purchased in Yancheng city, Jiangsu province, China. The average body length was 6.65 ± 0.50 cm and the average body mass was 4.81 ± 0.63 g of the individuals with similar size being selected for the experiment after 3 days of temporary feeding in the laboratory. We divided the crayfish into two groups: three animals were randomly selected as the experimental group and three as the control group. The former were treated with $20 \mu\text{L } K_2Cr_2O_7$ (0.001 g mL^{-1}) and the latter with $20 \mu\text{L PBS}$ [16]. Hepatopancreas tissues were collected after 24 h and frozen in liquid nitrogen then stored at -80°C until RNA extraction.

2.2. Total RNA extraction and detection

Total RNA from hepatopancreas tissues was extracted using Trizol reagent according to the manufacturer's instructions (Sangon, China). To ensure the use of qualified samples for transcriptome sequencing, the detection of the RNA included four methods as follows. RNA degradation and contamination were monitored using 1% agarose gels, purity of RNA was checked using a Nanodrop spectrophotometer, concentration was measured using a Qubit 2.0 fluorometer, and integrity was assessed using an Agilent 2100 Bioanalyzer.

2.3. Library construction and Illumina sequencing

Library construction was performed once high-quality RNA samples were obtained. First, oligo(dT)-attached magnetic beads were used to enrich the eukaryotic mRNA. Subsequently, the mRNA was randomly fragmented by fragmentation buffer. Using these short fragments as templates, first-strand cDNA was synthesized with random hexamer primers. The second strand of the cDNA was synthesized using RNase H and DNA polymerase I, and cDNA was then purified using AMPure XP. Purified double-stranded cDNA was then subjected to end-repair, followed by the addition of a tail and attachment of the sequencing connector. AMPure XP beads were used to select the fragment size. Finally, the cDNA library was obtained by PCR enrichment.

After the library construction was completed, we used the Qubit2.0 (Life Technologies, Carlsbad, CA) and Agilent 2100 (Agilent Technologies, Santa Clara, CA), respectively, to detect the concentration of the library and the insert size. The effective concentration of the library was accurately quantified using quantitative PCR (qPCR). Subsequently, the high-throughput sequencing platform Illumina

Table 1

Sequencing data for $K_2Cr_2O_7$ -treated and control samples.

Sample	Read Number	Base Number	GC Content	Q30(%)
PBS	22,067,581	6,589,701,420	53.79%	92.37%
Cr	25,566,472	7,654,577,926	36.91%	92.54%

Table 2

Assembled transcripts and unigenes obtained from *P. clarkii* hepatopancreas tissues via transcriptome analysis.

Length Range	Transcript	Unigene
200–300	10,825(24.16%)	9701(28.33%)
300–500	15,096(33.70%)	12,400(36.22%)
500–1000	11,189(24.98%)	7879(23.01%)
1000–2000	5422(12.10%)	3186(9.31%)
2000+	2.2655(5.06%)	1071(3.13%)
Total Number	44,797	34,237
Total Length	30,795,124	20,242,564
N50 Length	911	708
Mean Length	687.44	591.25

HiSeq, which can produce a large number of high-quality reads, was used to sequence the cDNA library.

2.4. Transcriptome assembly and functional annotation of unigenes

To obtain clean reads, we truncated the sequencing connector and primer sequences present in the raw reads, and also filtered low-quality sequencing data. Upon obtaining high-quality sequencing data, it needs to be sequentially assembled. Trinity is an assembly software designed specifically for high-throughput transcriptome sequencing [17]. Using Trinity, we first broke the reads into short fragments (K-mers). We then extended these short fragments into long ones (contigs) [18]. Taking advantage of an overlap between these fragments, we obtained a collection of fragments. Finally, the transcriptional sequence was identified in each fragment set using the method of De Bruijn mapping and sequencing the read information. BLAST was used to compare unigene sequences against the NCBI non-redundant protein (Nr) (<http://www.ncbi.nlm.nih.gov/>) [19,20], Swiss-Prot (a manually annotated and reviewed protein sequence database) (<http://www.ebi.ac.uk/uniprot/>) [21], Gene Ontology (GO) (<http://www.geneontology.org/>) [22], Clusters of Orthologous Groups of proteins/eukaryotic Orthologous Groups (COG/KOG) (<https://www.ncbi.nlm.nih.gov/COG/>) [23,24], eggNOG (database of orthologous groups of genes) (<http://eggnogdb.embl.de/>) [25], and Kyoto Encyclopaedia of Genes and Genomes (KEGG) (<http://www.genome.jp/kegg/>) [26]. KOBAS 2.0 was used to obtain KEGG Orthology results for unigenes in KEGG [27]. After predicting the amino acid sequence of unigenes, we used HMMER [28] to compare the unigene sequences with the Pfam [29] database to obtain annotation information on unigenes.

2.5. DEGs enrichment analysis

To identify DEGs between the two libraries, the calculation of unigene expression was performed using the fragments per kilobase of transcript per million fragments sequenced (FPKM) [30] method. This method was applied to compute the expression profiles of control and $K_2Cr_2O_7$ -treated hepatopancreas tissues [31]. The clean reads from each sample were mapped back onto the assembled transcriptome using the RSEM [32] software package. Read count for each gene was obtained from the mapping results. Before DEGs analysis, for each sequenced library, the read counts were adjusted using the edgeR program package through one scaling normalized factor [33]. Differential expression analysis of the two libraries was performed using DESeq R package [34]. The P-value was adjusted using the False Discovery Rate

Table 3
P. clarkii transcriptome annotation.

Anno Database	Annotated Number	300 ≤ length < 1000	length ≥ 1000	Percentage
COG Annotation	4668	2456	1256	32.87%
GO Annotation	6561	3611	1449	46.20%
KEGG Annotation	7065	3841	1705	49.75%
KOG Annotation	9245	5090	2143	65.10%
Pfam Annotation	9924	5381	2601	69.88%
Swissport Annotation	7376	3999	1969	51.94%
eggNOG Annotation	13144	7170	2764	92.55%
Nr Annotation	11989	6636	2833	84.82%
All Annotation	14202	7795	2913	

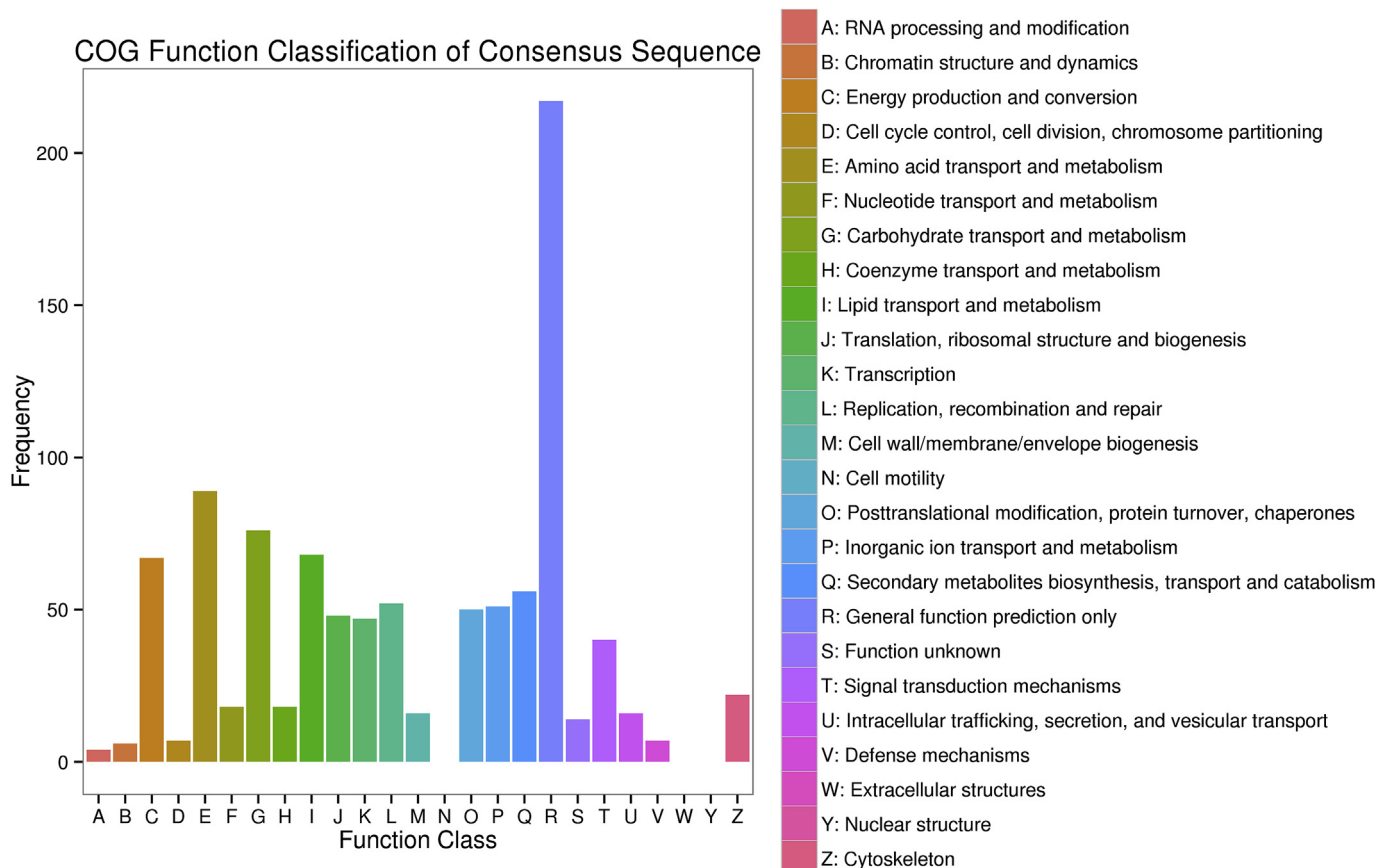


Fig. 1. Differential expression analysis of the assembled unigenes (control vs. $K_2Cr_2O_7$ -treated). The x-axis represents the fold-change between the control and $K_2Cr_2O_7$ -treated groups, and the y-axis indicates the significance of differential expression. Black Dots represent unigenes with no significant change, while red and green dots represent up and downregulated unigenes, respectively. (For interpretation of the references to colour in this figure legend, the reader is referred to the Web version of this article.)

Table 4
Number of differentially expressed genes identified in different functional databases.

DEG set	Annotated	COG	GO	KEGG	KOG	Pfam	Swiss-Prot	eggNOG	NR
PBS VS chrome	2233	729	996	1165	1479	1860	1360	2026	2144

(FDR) [35,36]. $FDR < 0.01$ and $|\log_2(\text{fold change})| > 2$ were set as the threshold for significantly differential expression. GO functional enrichment and KEGG pathway analyses of DEGs were subsequently performed using GOSec R and KOBAS, respectively [37].

2.6. Identification of simple sequence repeats (SSRs) and single nucleotide polymorphism (SNP) sites

SSRs were identified using MISA software. Reads and unigenes

sequences for each sample were compared using STAR [38], and SNP sites were identified using GATK's SNP identification (SNP calling) [39] process for RNA-Seq.

2.7. Quantitative real-time PCR (qRT-PCR)

To verify the expression level of the most promising candidate genes, we performed qRT-PCR using 10 genes that were randomly selected from common DEGs. Gene-specific primers were designed using

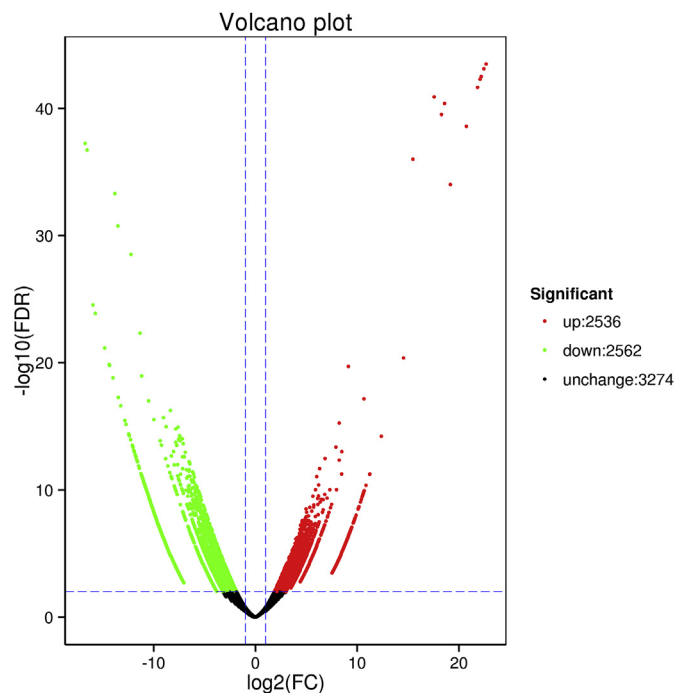


Fig. 2. Differentially expressed genes between the two groups and annotation results of all genes at level 2 under the three main GO categories.

Primer 5.0. The synthesized cDNA was used as a template; qRT-PCR was performed using a TUREscript cDNA Synthesis Kit (Aidlab, China), following the manufacturer's instructions. The 18S rRNA gene was used as an internal reference gene. qRT-PCR was performed using a Mastercycle EP Realplex (Eppendorf, Germany) with a $2 \times$ SYBR Green qPCR Mix Kit (Aidlab, China) in the following conditions: 95 °C for 30 s, followed by 40 cycles of 95 °C for 30 s, 58 °C for 25 s, and 72 °C for 25 s. Each independent experiment was performed in triplicate, and the relative expression level of a gene was determined using the $2^{-\Delta\Delta CT}$ method [40]. Mean \pm standard error (standard error of mean, SEM) is used to report the data. Three replicate reactions per sample were used to ensure statistical credibility.

3. Results and discussion

3.1. Assembly and splicing

A total of 25,566,472 and 22,067,581 clean reads were obtained from $K_2Cr_2O_7$ -treated and control samples, giving rise to total clean base numbers of 7 654,577,92 and 6,589,701,42 respectively. Q30 was $> 92\%$, and the G + C content was approximately 37% in $K_2Cr_2O_7$ -treated samples and 54% in control samples (Table 1). Using Trinity software, 44,797 transcripts were generated with average length of 687.44 bp and N50 length of 911 bp; 34,237 unigenes were identified with mean length of 591.25 bp and N50 length of 708 bp. Among these unigenes, 22,101 (64.55%) were 200–500 bp long; 7879 (23.01%) were 500–1000 bp; 3186 (9.31%) were 1–2 kbp; and 1071 (3.13%) were > 2 kbp (Table 2). These results show that the data were of high quality and that unigenes could be used for annotation analysis.

3.2. Functional annotation and classification

To obtain comprehensive gene function information, we used eight databases to annotate unigenes: Nr, KEGG, COG, Swiss-Prot, eggNOG, Pfam, GO and KOG. In total, 34,237 unigenes were annotated as follows: 11,989 in Nr (84.42%); 7065 in KEGG (49.75%); 4668 in COG (32.87%); 7376 in Swiss-Prot (51.94%); 13,144 in eggNOG (92.55%);

9924 in Pfam (69.88%); 6561 in GO (46.20%); and 9245 in KOG (66.36%) (Table 3). On the basis of our differential expression analysis, 5098 significant DEGs were identified between $K_2Cr_2O_7$ -treated and control samples; of these DEGs, 2536 were up-regulated (Table S1) and 2562 were down-regulated DEGs (Table S2) (Fig. 1). Volcano plots can intuitively show the relationship between FDR and fold-change of all genes to depict the degree of difference in gene expression level and its statistical significance between the two groups of samples. As evident from Fig. 1, the expression pattern of unigenes seems to have a specific relationship with Cr (VI) stimulation.

3.3. Identification and enrichment analysis of DEGs

The number of DEGs identified in different functional databases were 729 in COG, 996 in GO, 1165 in KEGG, 1479 in KOG, 1860 in Pfam, 1360 in Swiss-Prot, 2026 in eggNOG, and 2144 in Nr (Table 4). All DEGs were classified into three categories according to topGO, including “biological process” (BP), “cell component” (CC) and “molecular function” (MF). Among the various categories of BP, “metabolic process,” “cellular process,” and “single-organism process” were the top three. In the CC category, it was “cell,” “cell part,” and “organelle” that dominated. In the MF class, the two main ones were “catalytic activity” and “binding” (Fig. 2). In the COG database, 729 unigenes were classified. Through the classification of DEGs in COG, we found that the “general function prediction” class had the highest frequency (Fig. 3). All KEGG annotation pathways are shown in Fig. 4. Four of these pathways were related to cellular processes, four to environmental information processing, and seven to genetic information processing. Finally, there were 34 pathways involved in metabolism. Although no clear molecular mechanisms have been identified so far to counter Cr toxicity, some unigenes with different expression levels could be elucidated through annotation and classification.

3.4. Identification of SSRs and SNPs

We used MISA to identify potential SSRs. A total of six SSR types were identified: mono-, di-, tri-, tetra-, penta-, and hexanucleotide SSRs. A total of 1877 SSRs were identified in the final analysis. Among them, the most abundant SSR type was mononucleotide (913), followed by di- (476), tri- (347), penta- (131), tetra- (8), and hexanucleotide (1) SSRs (Table 5). According to the number of alleles at SNP loci, namely the number of different bases supported by sequencing reads, SNP loci can be divided into HomoSNP loci (only one allele) and HeteSNP loci (two or more alleles). A total of 21,292 SNPs were detected in the $K_2Cr_2O_7$ -treated group, of which 8248 were HomoSNP and 13,044 were HeteSNP, and 18,904 SNPs were detected in the control group, of which 8511 were the HomoSNP and 10,393 were HeteSNP (Table 6). Potential SNPs and SSRs found in our transcriptome datasets may provide important information about the response of *P. clarkii* to oxidative stress.

3.5. Pathways related to antioxidant defense

Fig. 5 shows the peroxisome pathway, which is associated with the antioxidant system. In this pathway, peroxin-14 (PEX14), Mpv17-like protein (MPV17), 2-hydroxyacyl-CoA lyase 1 (HPC12), acyl-CoA oxidase (ACOX), sterol carrier protein-2 (SCPX), bile acid-CoA: amino acid N-acyltransferase (BAAI), 4-dienoyl-CoA isomerase (ECH), peroxisomal trans-2-enoyl-CoA reductase (PECR), long-chain acyl-CoA synthetase (ACSL), carnitine O-octanoyltransferase (CROT), alkyldihydroxyacetonephosphate synthase (AGPS), alcohol-forming fatty acyl-CoA reductase (FAR), D-amino-acid oxidase (DAO), D-aspartate oxidase (DDO), CAT, SOD, GST kappa-1 (GSK1), and xanthine dehydrogenase/oxidase (XDH) are associated with the down-regulated genes, whereas carnitine O-acetyltransferase (CRAT), peroxiredoxin 5, and atypical 2-Cys peroxiredoxin (PRDX5) are associated with the up-regulated genes. The main functions of peroxidases are fatty acid oxidation and ether

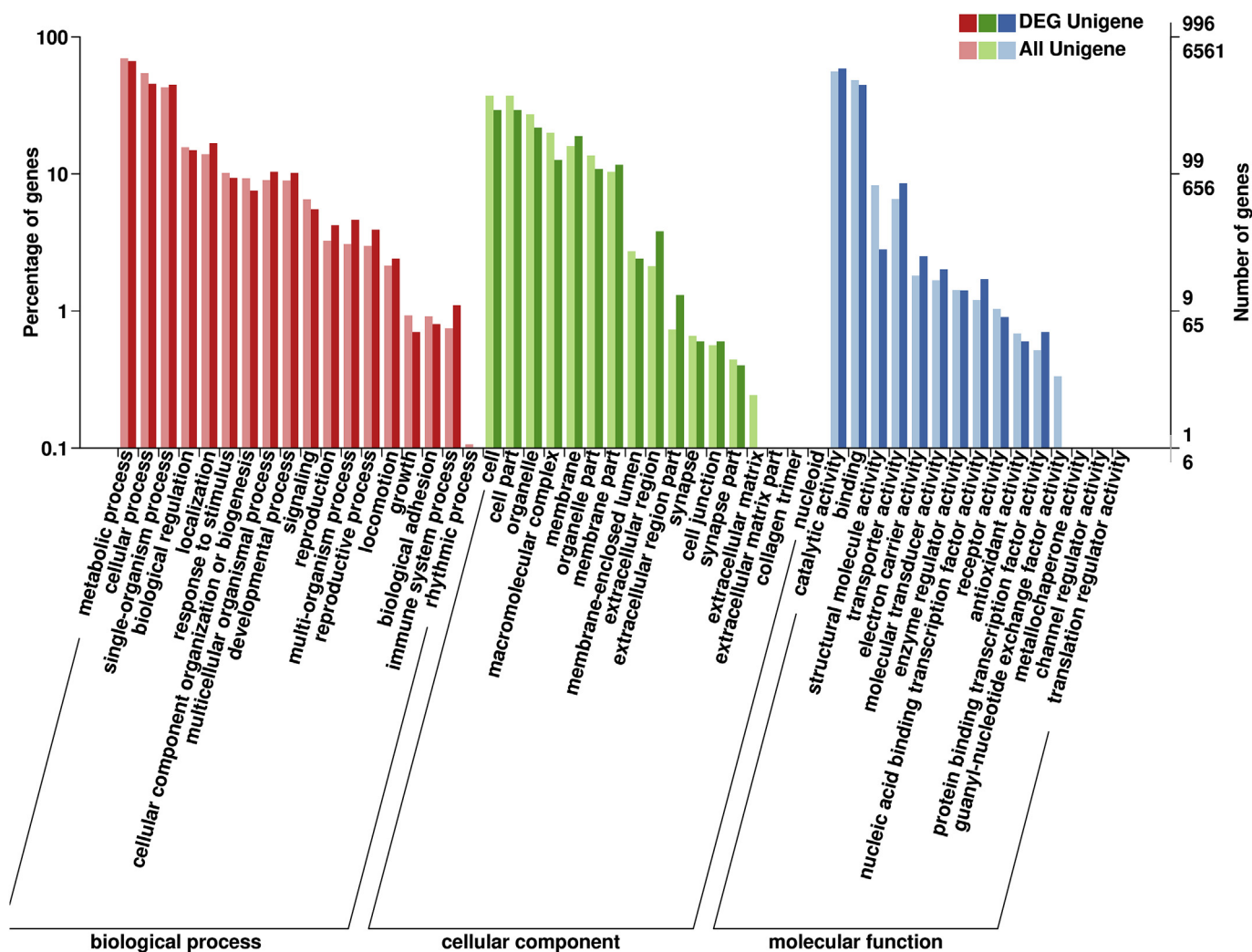


Fig. 3. Classification of differentially expressed genes in Clusters of Orthologous Groups of proteins.

phospholipid biosynthesis. They also play an important role in the antioxidant system, including in hydrogen peroxide (H₂O₂) and glutathione metabolism. CAT and SOD are produced in the metabolic process of H₂O₂. They are two related antioxidant enzymes, which can together remove reactive oxygen radicals and protect organisms from oxidative damage [41,42]. CAT is a scavenger enzyme and can promote H₂O₂ decomposition into molecular oxygen and water so as to protect cells from being poisoned. This experiment showed that CAT activity level was inhibited in the presence of heavy metal ions, which is contradictory to the results of other studies on the effect of pollutants on CAT activity levels in crayfish [43]. This is because when crayfish are exposed to Cr (VI) for a long time at a high concentration, their body produces more oxidative substances than their defense ability can deal with, which leads to structural and functional damage and decreased CAT activity levels. A large amount of H₂O₂ is produced in crayfish after the action of heavy metal ions, which disturbs the antioxidant defense system. Changes in CAT activity levels can be used to evaluate heavy metal ion toxicity by monitoring by the detoxification mechanism of *P. clarkii*.

3.6. Validation of transcriptome data by qRT-PCR

To verify the expression level of the most promising candidate genes identified in our transcriptome analysis, 10 DEGs were randomly selected for qRT-PCR analysis at 24 h after Cr (VI) treatment. All 10 genes were variably expressed in comparison to the control group (Fig. 6).

Among them, heat shock protein 70 (HSP70) and lectin displayed the highest expression levels, followed by Kazal SPI, thioredoxin, copper/zinc SOD isoform (Cu/ZnSOD), FK506-binding nuclear protein (FK506), cathepsin and lipase. Catalase and hemocyanin displayed the lowest expression levels.

When crayfish are subjected to Cr (VI) stress, they will produce a large number of HSPs, which are considered as a kind of conservative proteins. The application value of HSPs in immunology is attracting more and more attention. HSP70 is the most abundant of the HSPs strong immunogenicity. It is the main target molecule of the immune system and can be expressed in large quantities in response to Cr (VI) stress. Therefore, HSP70 can be used as an indicator to determine the stress state in crayfish. Lectins are class of proteins that can bind specific sugar molecules and play an important role in immune recognition and response. C-type lectin is an important pattern recognition receptor in crustaceans. Furthermore, lectin stimulates apoptotic signaling, and it plays an important role in immune responses. Together, these immune-related DEGs could play an important role in the immune defenses.

4. Conclusion

In this study, we characterized the transcriptome of *P. clarkii* using RNA sequencing method and performed a comparison between K₂Cr₂O₇-treated samples and controls. Unigenes were annotated by seven databases. In total, 5098 significant DEGs were found, including

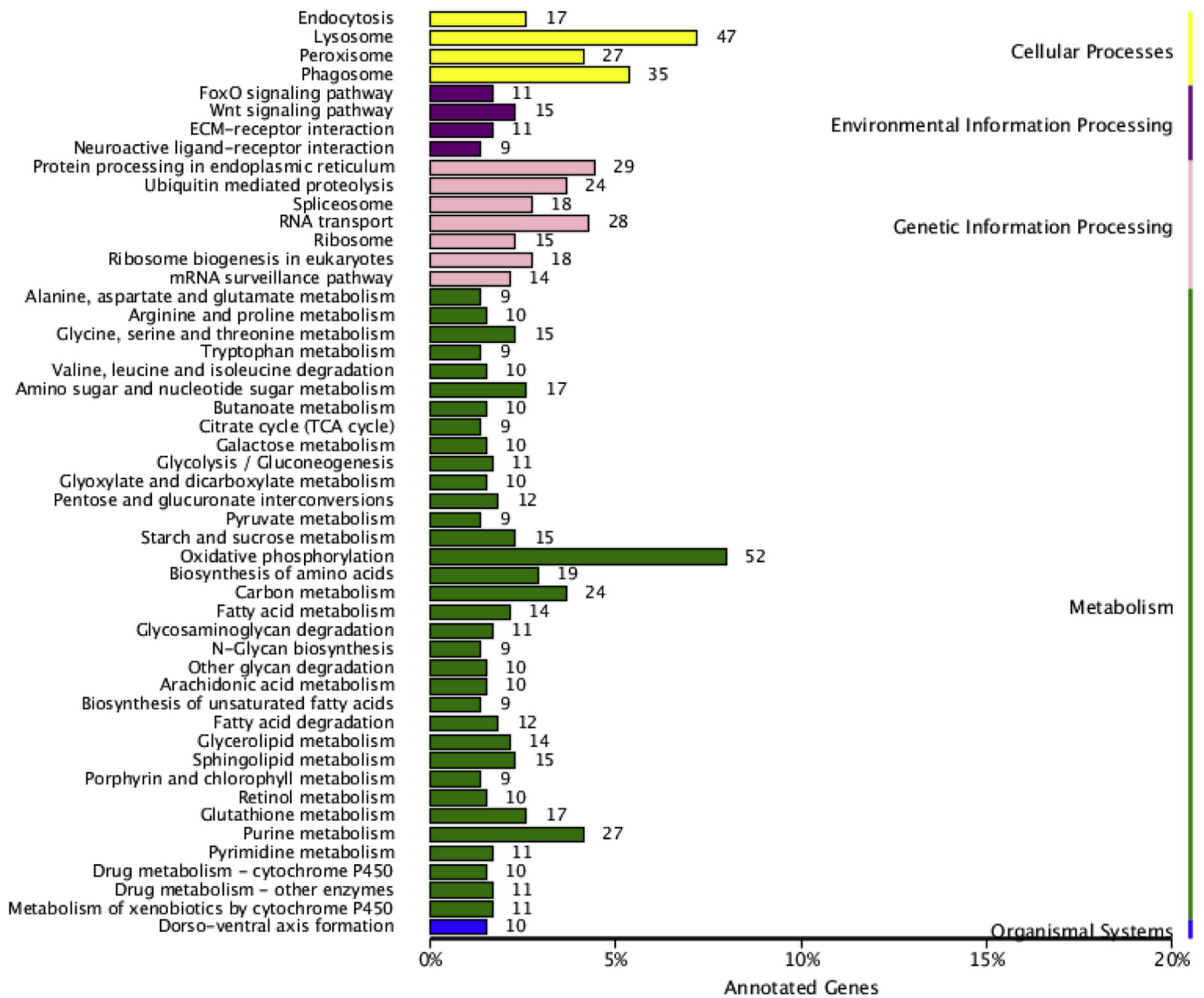


Fig. 4. Annotation results of differentially expressed genes classified according to KEGG pathways. The ordinate shows the names of KEGG metabolic pathways, and the abscissa shows the proportion of the number of genes annotated into the pathway.

Table 5

Distribution of various types of simple sequence repeat.

Type	compound repeat SSR	single base repeat SSR	double base repeat SSR	three-base repeat SSR	four-base repeat SSR	six-base repeat SSR
Number	131	913	476	347	8	1

Table 6

Distribution of various types of single nucleotide polymorphism.

Sample	HomoSNP	HeteSNP	AllSNP
PBS	8248	13044	21292
Cr	8511	10393	18904

2536 and 2562 that were significantly up- and downregulated, respectively. We found that heavy metal ions had obvious effects on the antioxidant system in *P. clarkii*. This system plays an important role in conferring protection against oxidative damage. Enzymes such as CAT and SOD can remove reactive oxygen species and prevent oxidative damage. When crayfish encounter high concentrations of Cr (VI) for a long duration, their body produces more oxidants than their defense

ability can resolve, which leads to structural and functional damage and decreased CAT activity levels. qRT-PCR analysis showed that DEGs related to immune system contribute to the immune response of *P. clarkii*. In conclusion, our results contribute to understanding of the antioxidant defense system used by *P. clarkii* in response to heavy metal stress.

Acknowledgements

This work was supported by the Natural Science Foundation of Jiangsu Province (BK20160444), the National Natural Science Foundation of China (31640074), the Zhejiang Provincial Natural Science Foundation of China (LY19B020012 and LY19H160015), the Jiangsu Agriculture Science and Technology Innovation Fund (CX(18)

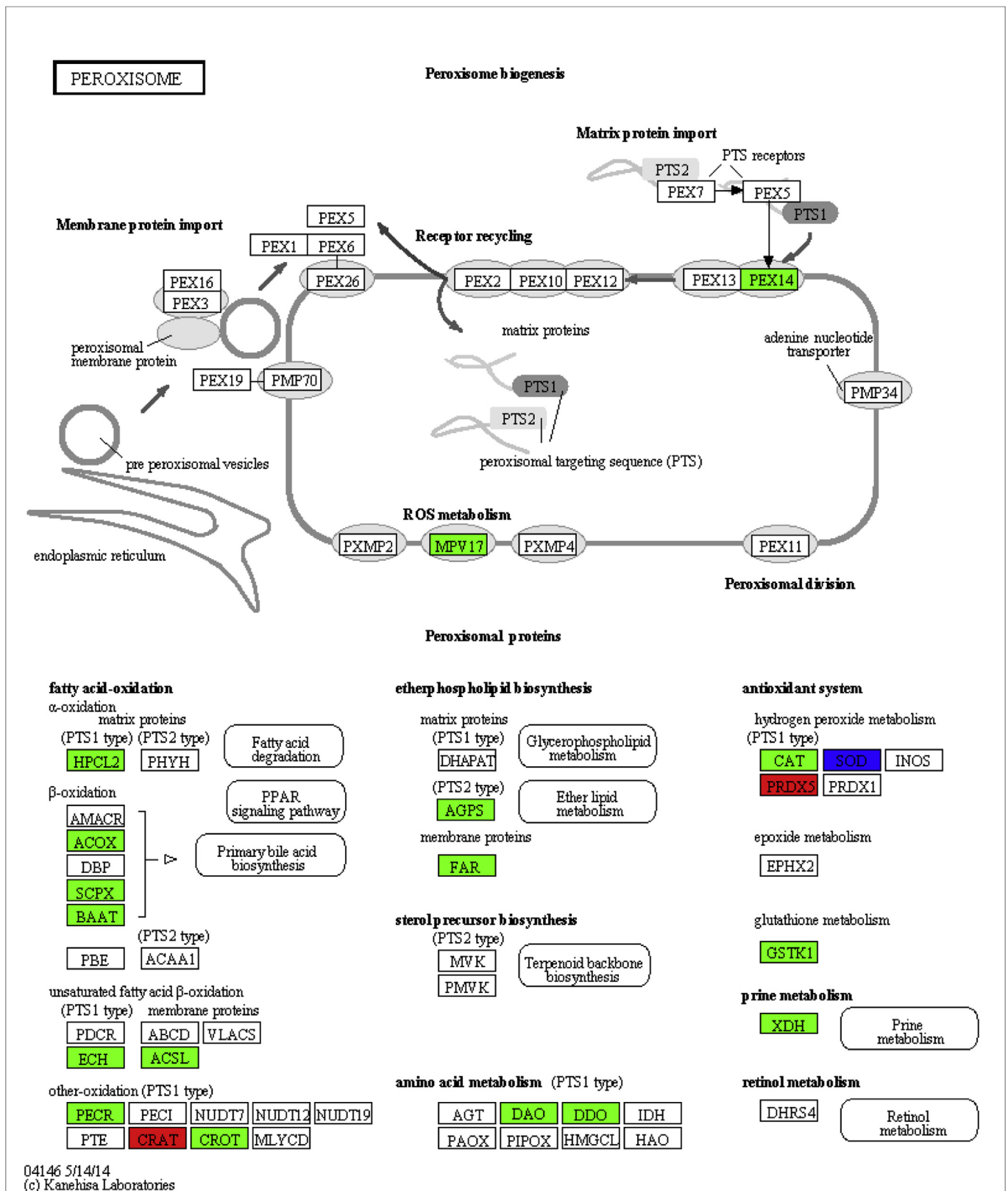


Fig. 5. The peroxisome pathway. Enzymes enclosed in the red and blue boxes were associated with upregulated genes and those in the green box were associated with downregulated genes. (For interpretation of the references to colour in this figure legend, the reader is referred to the Web version of this article.)

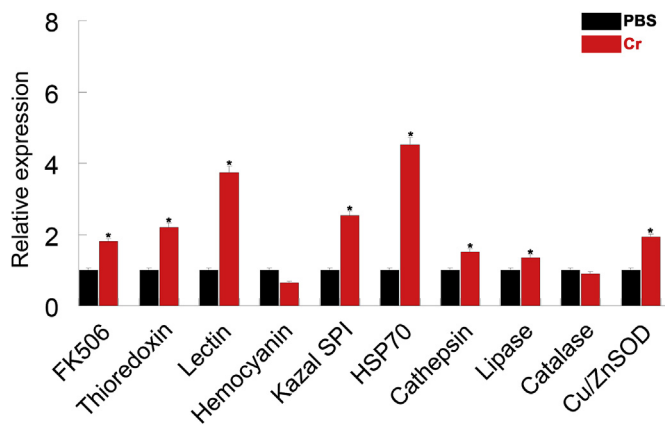


Fig. 6. qRT-PCR results showing relative expression profiles of 10 randomly selected immune response-associated genes following Cr (VI) stimulation. The 18S rRNA gene was used as an internal reference. Gene expression levels in the control group were set as 1.0. Data are expressed as mean fold-change (mean \pm standard error, $n = 3$) relative to the control group.

3027), and sponsored by Qing Lan Project of Jiangsu Province. The authors declare no competing interests.

Appendix A. Supplementary data

Supplementary data to this article can be found online at <https://doi.org/10.1016/j.fsi.2018.12.055>.

References

- [1] F. Baruthio, Toxic effects of chromium and its compounds, *Biol. Trace Elem. Res.* 32 (1992) 145–153.
- [2] P.B. Tchounwou, C.G. Yedjou, A.K. Paylolla, et al., Heavy metal toxicity and environment, in: A. Luch (Ed.), *Molecular, Clinical and Environmental Toxicology*, 32 Experiential Supplementum Springer Basel AG, Switzerland, 2012, pp. 133–164.
- [3] S.J. Stoh, D. Bagchi, Oxidative mechanisms in the toxicity of metal ions, *Free Radic. Biol. Med.* 18 (1995) 321–336.
- [4] F. Baruthio, Toxic effects of chromium and its compounds, *Biol. Trace Elem. Res.* 32 (1992) 145–153.
- [5] M.M. Aruldas, S. Subramanian, P. Sekar, et al., Chronic chromium exposure-induced changes in testicular histoarchitecture are associated with oxidative stress: study in a non-human primate (*Macaca radiata* Geoffroy), *Hum. Reprod.* 20 (2005) 2801–2813.
- [6] Z.H. Jia, M.Q. Wang, X.D. Wang, et al., Identification of a clip domain serine proteinase involved in immune defense in Chinese mitten crab *Eriocheir sinensis*, *Fish Shellfish Immunol.* 74 (2018) 332–340.
- [7] H. Jiang, Y.M. Cai, L.Q. Chen, et al., Functional annotation and analysis of expressed sequence tags from the hepatopancreas of mitten crab (*Eriocheir sinensis*), *Mar. Biotechnol.* 11 (2009) 317–326.
- [8] Y.C. Gai, J.M. Zhao, L.S. Song, et al., Two thymosin-repeated molecules with structural and functional diversity coexist in Chinese mitten crab *Eriocheir sinensis*, *Dev. Comp. Immunol.* 33 (2009) 867–876.
- [9] T.K.S. Janssens, D. Roelofs, N.M. Van Straalen, et al., Molecular mechanisms of heavy metal tolerance and evolution in invertebrates, *Insect Sci.* 16 (2009) 3–18.
- [10] Z.Z. Xin, Q.N. Liu, Y. Liu, et al., Transcriptome-wide identification of differentially expressed genes in Chinese oak silkworm *Antheraea pernyi* in response to Lead challenge, *J. Agric. Food Chem.* 65 (2017) 9305–9314.
- [11] J.C. Marioni, C.E. Mason, S.M. Mane, et al., RNA-seq: an assessment of technical reproducibility and comparison with gene expression arrays, *Genome Res.* 18 (2008) 1509–1517.
- [12] Z.H. Jia, M.Q. Wang, X.D. Wang, et al., Transcriptome sequencing reveals the involvement of reactive oxygen species in the hematopoiesis from Chinese mitten crab *Eriocheir sinensis*, *Dev. Comp. Immunol.* 82 (2018) 94–103.
- [13] U. Nagalakshmi, The transcriptional landscape of the yeast genome defined by RNA sequencing, *Science* 320 (2008) 1344–1349.
- [14] M. Xu, L. Jiang, K.N. Shen, et al., Transcriptome response to copper heavy metal stress in hard-shelled mussel (*Mytilus coruscus*), *Genomics Data* 7 (2016) 152–154.
- [15] X. Meng, X. Tian, G. Ni, et al., The transcriptomic response to copper exposure in the digestive gland of Japanese scallops (*Mizuhopecten yessoensis*), *Fish Shellfish Immunol.* 46 (2015) 161–167.
- [16] Q.N. Liu, Z.Z. Xin, Y. Liu, et al., A ferritin gene from *Procambarus clarkii*, molecular characterization and in response to heavy metal stress and lipopolysaccharide challenge, *Fish Shellfish Immunol.* 63 (2017) 297–303.
- [17] H.S. Shen, Y.C. Hu, Y.C. Ma, et al., In-depth transcriptome analysis of the red swamp crayfish *Procambarus clarkii*, *PLoS One* 9 (2014) e110548.
- [18] M.G. Grabherr, B.J. Haas, M. Yassour, et al., Full-length transcriptome assembly from RNA-Seq data without a reference genome, *Nat. Biotechnol.* 29 (2011) 644–652.
- [19] S.F. Altschul, T.L. Madden, A.A. Schffer, et al., Gapped BLAST and PSI BLAST: a new generation of protein database search programs, *Nucleic Acids Res.* 25 (1997) 3389–3402.
- [20] Y.Y. Deng, J.Q. Li, S.F. Wu, et al., Integrated nr database in protein annotation system and its localization, *Computer Engineering Italic* 32 (2006) 71–74.
- [21] R. Apweiler, A. Bairoch, C.H. Wu, et al., UniProt: the universal protein knowledgebase, *Nucleic Acids Res.* 32 (2004) 115–119.
- [22] M. Ashburner, C.A. Ball, J.A. Blake, et al., Gene ontology: tool for the unification of biology, *Nat. Genet.* 25 (2000) 25–29.
- [23] R.L. Tatusov, M.Y. Galperin, D.A. Natale, The COG database: a tool for genome scale analysis of protein functions and evolution, *Nucleic Acids Res.* 28 (2000) 33–36.
- [24] E.V. Koonin, N.D. Fedorova, J.D. Jackson, et al., A comprehensive evolutionary classification of proteins encoded in complete eukaryotic genomes, *Genome Biol.* 5 (2004) R7.
- [25] J. Huerta-Cepas, D. Szklarczyk, K. Forslund, et al., eggNOG 4.5: a hierarchical orthology framework with improved functional annotations for eukaryotic, prokaryotic and viral sequences, *Nucleic Acids Res.* 35 (2015) 1248.
- [26] M. Kanehisa, S. Goto, S. Kawashima, et al., The KEGG resource for deciphering the genome, *Nucleic Acids Res.* 32 (2004) 277–280.
- [27] C. Xie, X. Mao, J. Huang, et al., KOBAS 2.0: a web server for annotation and identification of enriched pathways and diseases, *Nucleic Acids Res.* 39 (2011) 316–322.
- [28] S.R. Eddy, Profile hidden Markov models, *Bioinformatics* 14 (1998) 755–763.
- [29] R.D. Finn, A. Bateman, J. Clements, et al., Pfam: the protein family database, *Nucleic Acids Res.* 56 (2013) 1223.
- [30] C. Trapnell, B.A. Williams, G. Pertea, et al., Transcript assembly and quantification by RNA Seq reveals unannotated transcripts and isoform switching during cell differentiation, *Nat. Biotechnol.* 28 (2010) 511–515.
- [31] L.S. Dai, M.N. Abbas, S. Kausar, et al., Transcriptome analysis of hepatopancreas of *Procambarus clarkii* challenged with polyribinosinic polyribocytidylic acid (poly I:C), *Fish Shellfish Immunol.* 71 (2017) 144–150.
- [32] B. Li, N.D. Colin, RSEM: accurate transcript quantification from RNA Seq data with or without a reference genome, *BMC Bioinf.* 12 (2011) 323.
- [33] M. Zhou, M.N. Abbas, S. Kausar, et al., Transcriptome profiling of red swamp *P. clarkii* (*Procambarus clarkii*) hepatopancreas in response to lipopolysaccharide (LPS) infection, *Fish Shellfish Immunol.* 71 (2017) 423–433.
- [34] S. Anders, W. Huber, Differential expression analysis for sequence count data, *Genome Biol.* 11 (2010) 106.
- [35] J.D. Storey, The positive false discovery rate: a Bayesian interpretation and the q-value, *Ann. Stat.* 31 (2003) 2013–2035.
- [36] C.Z. Liu, X. Wang, J.H. Xiang, et al., EST-derived SNP discovery and selective pressure analysis in Pacific white shrimp (*Litopenaeus vannamei*), *Chin. J. Oceanol. Limnol.* 30 (2012) 713–723.
- [37] M. Kanehisa, M. Araki, S. Goto, et al., KEGG for linking genomes to life and the environment, *Nucleic Acids Res.* 36 (2008) 480–484.
- [38] G.A. Auwera, M.O. Carnerio, C. Hartl, et al., From FastQ data to high confidence variant calls: the genome analysis toolkit best practices pipeline, *Curr. Protocols Bioinforma.* 63 (2013) 11–10.
- [39] A. Dobin, C.A. Davis, F. Schlesinger, et al., STAR: ultrafast universal RNA-seq aligner, *Bioinformatics* 29 (2013) 15–21.
- [40] K.J. Livak, T.D. Schmittgen, Analysis of relative gene expression data using realtime quantitative PCR and the 2⁻(Delta Delta C_T) Method, *Methods* 25 (2001) 402–408.
- [41] H.N. Kirkman, G.F. Gaetani, Mammalian catalase: a venerable enzyme with new mysteries, *Trends Biochem. Sci.* 32 (2007) 44–50.
- [42] M. Islinger, K.W. Li, J. Seitz, et al., Hitchhiking of Cu/Zn superoxide dismutase to peroxisomes-evidence for a natural piggyback import mechanism in mammals, *Traffic* 10 (2009) 1711–1721.
- [43] Y. Liu, Z.Z. Xing, J. Song, et al., Transcriptome analysis reveals potential anti-oxidant defense mechanisms in *Antheraea pernyi* in response to Zinc stress, *J. Agric. Food Chem.* 66 (2018) 8132–8141.